PCCP

Complex vibrational correlation functions extracted from the resolved ν_2 band of liquid acetonitrile

Dmitry Nerukh†[a] and Trevor R. Griffiths*[b]

[a] *Department of Chemistry, University of Nevada, Reno, NV 89557, USA*
[b] *School of Chemistry, University of Leeds, Leeds, UK LS2 9JT*

Received 27th November 2000, Accepted 15th March 2001
First published as an Advance Article on the web 6th April 2001

The development of a sophisticated model is presented for fitting the experimental Raman spectra of liquid acetonitrile. A new approach for extracting all possible band shape details of highly overlapping spectral bands is derived and implemented. A unique, statistically justified resolution is obtained of the ν_2 vibrational band into its components at 25, 50 and 75 °C. The parameters of both the real and imaginary parts of the vibrational correlation functions are reported for the first time together with their confidence intervals. The quantitative characteristics obtained of the ν_2 mode dynamics can be considered as experimental data and used for testing theoretical models of vibrational relaxation.

Introduction

The vibrational spectra of liquids contain information concerning the dynamics of the molecules of that liquid. Extracting that information is difficult because many processes, including rotational and vibrational relaxation, are taking place simultaneously therein and thus contribute to the observed spectra. However, it is possible to derive the dynamic data of molecules in the liquid state if the quality and accuracy of experimental data is of the best and a unique resolution of the spectra into its component bands can be performed. We recently demonstrated[1] that this could be achieved, using a range of varied examples, and used the term 'unique resolution' to mean that spectra can be resolved unambiguously within a chosen theoretical model. We retain that usage here and assume familiarity with that publication.[1]

Our approach requires that we choose (or construct) an appropriate theoretical model for the shapes of the constituent bands (often referred to as line shapes) that is based upon two factors. The first comprises the existing theoretical considerations concerning the dynamics of the molecules when in the liquid state, and the second relates to the ability to use the theoretical model to obtain a unique resolution of the spectra.

We therefore here describe the methodology of the construction of the model that allows us to extract *all* the line shape information from highly overlapping bands while retaining the framework of a carefully analysed theoretical model. Specifically, the Raman spectrum of liquid acetonitrile is analysed. The emerging vibrational correlation functions of the ν_2 mode at different temperatures are obtained and detailed information about their shape, together with the confidence intervals of their parameters, is presented.

Statistically justified resolution of experimental spectra into band shapes

The computer program that provides a unique resolution has been published.[1] The requirements of the associated model are that it should be adequate and able to reproduce all the features of the spectrum, and also not too complex, but simple enough to ensure that a unique resolution of the spectrum is obtained.

The resolution procedure employs a least-squares fitting in which regression analysis formalism is used. Hence it is assumed that an experimental spectrum can be represented by $y(\boldsymbol{X}) = \eta(\boldsymbol{X}) + \varepsilon$. The experimental y values here depend on a set of unknown parameters $\boldsymbol{X}$, and are considered as a random variable that is the sum of its expectation value η and purely random deviation ε. A further assumption is the equivalence between $\eta(\boldsymbol{X})$ and some predefined theoretical model $y^{\text{theor}}(\mathbf{X})$:

$$\eta = y^{\text{theor}}. \tag{1}$$

A least-squares procedure is then applied to obtain the values of the parameters $\boldsymbol{X}$.

This process is often not taken further in the derivation of $\boldsymbol{X}$ parameters. However, such incomplete regression analysis processes may easily lead to erroneous conclusions. To avoid this possibility the following two procedures are performed.

(a) The chosen theoretical model is checked for correctness, in that assumption (1) is fulfilled. This can be achieved by analysing the properties of the calculated ε values. Rigorously, the values $\varepsilon_i^{\chi} = \varepsilon_i/\sigma_i$ at each experimental point (each wavenumber), where σ_i are experimental dispersions, are all normally distributed random variables with mean zero and equal standard deviations. The sum of squares of these values over the experimental points is χ^2, the distributed random variable. The numerical values of χ^2 for truly normally distributed random ε_i^{χ} are tabulated or can easily be calculated for each of the number of degrees of freedom (the difference between the number of experimental points and the number of fitting parameters). It is then possible to compare the tabulated χ^2 values with that calculated from a particular fit under investigation. If these values are too different (and there is a statistically justified way of expressing the extent of their equivalence) that means that ε_i^{χ} values are not normally distributed with a zero mean and the same standard deviation. Hence, assumption (1) is not fulfilled, the theoretical model is incorrect and the whole fit has no meaning.

However, there is a subtle point in the outlined procedure. The final χ^2 is rather sensitive to the experimental dispersions σ_i. Thus, unless accurate σ_i are known, the results of such an analysis cannot be considered reliable. Nevertheless, ε_i values

† Present address: Department of Chemistry, University of Cambridge, Lensfield Road, Cambridge, UK CB2 1EW.

can be analysed directly. While the standard deviations of the ε_i distributions are not equal, the mean still should be zero. Hence, if the differences $y - y^{theor}$ show a regular trend this indicates that the model y^{theor} is insufficiently complex because ε is not purely random. The problem of defining a proper model y^{theor} is considered below and its application to a real spectrum is discussed later.

(b) A unique least-squares solution must be obtained. While normally unique in the case of a linear model in the non-linear case this can be a particularly difficult problem, especially when a complex model is used, as is often the case for the resolution of spectra. This question has been earlier analysed in detail.[1]

Only if these two conditions are fulfilled are the values of the parameters $\boldsymbol{X}$ meaningful, and their confidence intervals can then be reliably calculated. From among the various methods for calculating confidence intervals the Monte Carlo method is one of the most general and reliable[2] and used here.

Goodness-of-fit

When defining the model there are two situations to avoid. These are schematically illustrated in Fig. 1 for the case of the simplified one-parameter fit. Too simple an approach can result in an underestimated model, as represented in Fig. 1a, and too elaborate an approach will yield an overestimated model, typified in Fig. 1c. An acceptable situation corresponds to Fig. 1b. The quantitative measure for the goodness-of-fit is given by the probability Q that the chi-square should exceed a particular value χ^2 by chance[2] (see above). For the underestimated model this probability is considerably less then unity: in the overestimated case its value is very close to unity. If the model is optimal, the Q value lies between $\sim 1 \times 10^{-2}$ and ~ 0.9.[2]

When the minimum of the sum of squares of deviations (SSD) is calculated then one of the possible profiles shown in Fig. 1d, e, f is obtained. Here D roughly corresponds to the experimental dispersion that is the value to which the calculated dispersion of approximation, SSD/(the number of degrees of freedom), should correspond. In reality, each experimental point has its own D value that is impossible to plot, and strictly the behaviour of Q should be analysed. It is thus important that the goodness-of-fit should be as close to the ideal situation (Fig. 1b, e) as possible, because otherwise subsequent manipulations will not produce meaningful results.

In reality the situation is often even worse. The model may be quite elaborate and hence the plot of the sum of squares of deviations against the parameter value shows a profile like that of the overestimated model, but unfortunately all its minima are still greater than the experimental dispersion (Fig. 1g), as in the underestimated model. We here have the features of both unacceptable cases.

To obtain statistically justified parameters this type of situation should be avoided. From the statistical point of view, the overestimated model (Fig. 1c, f) is also acceptable, but it is generally not acceptable in the sense of fitting a unique solution (condition (b) above).

Confidence intervals

In the calculation of confidence intervals for the parameters of a somewhat sophisticated non-linear model the process is not straightforward. The profile obtained, as in Fig. 1g, at no point crosses the D value or, equivalently, the Q value is considerably less then unity. This situation does not produce confidence intervals, and thus here all the values of the fitting parameter obtained are invalid.

Even when the acceptable situation is achieved (Fig. 1b, e), the calculation of the confidence intervals for the parameters should be carried out with care. Attempts to obtain them in the global minimum using standard gradient methods are not useful, because they produce the confidence intervals of local

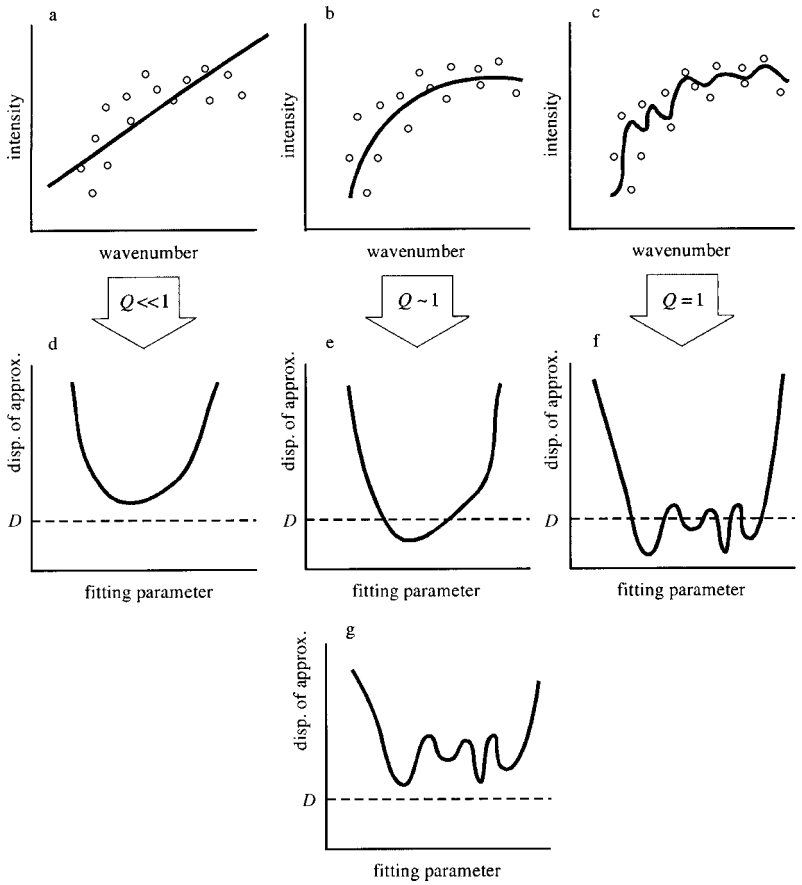

Fig. 1 Various theoretical models (a, b and c) and the corresponding schematic behaviour of the minimising function (dispersion of approximation—see text) (d, e, f and g) for the one-dimensional model case. D denotes generalised "experimental dispersion".

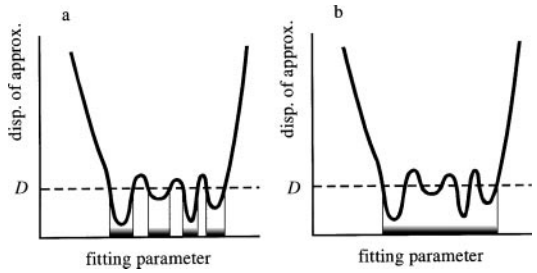

Fig. 2 Confidence intervals of a generalised parameter. (a), Rigorous definition; (b), commonly used approximation. D denotes generalised "experimental dispersion".

minima. Also, the minimising function is assumed to be approximated by the quadratic form and this cannot be applied in the general case for complex non-linear models.

Ideally, the ranges of the acceptable values of the parameter are those where the approximation dispersion is less then the experimental dispersion (strictly, Q is in the acceptable range). The one-dimensional case is illustrated in Fig. 2a. In higher dimensional space this region can be of a more complicated shape. For simplicity, however, these ranges can be approximated and reduced to a single section (Fig. 2b): in the higher dimensional space of the optimising parameters the approximation would be an ellipsoid. Again, the general algorithm for finding these confidence intervals uses the Monte Carlo simulation that employs the generation of the 'fictitious' experimental data set and fits these data to accumulate statistics on the fitting parameters.[2]

Specialised approach for extracting line shapes from highly overlapping spectral bands

Current theoretical models of liquids employ complex line shapes[3–5] that are almost always non-linear. Even though the resulting line shape may be very complex, involving up to 10 parameters, we have found (see later) that it proved difficult and sometimes impossible to obtain the acceptable situation represented in Fig. 1b, e. We have therefore devised a new approach that overcomes this problem by using a combination of a non-linear and a linear fit. This process allows line shapes to be obtained from the overlapping bands. These shapes are extracted from the experimental spectra and based on general theoretical considerations. Certain assumptions are contained in the process but they are of a general nature and thus the method should be applicable to a wide range of experimental spectra. The algorithm is as follows:

(1) Fit the spectrum with bands of the non-linear shape dictated by one of the theories. The band shapes should be elaborate enough to reproduce the main features of the spectrum.

(2) Calculate the differences between the experimental and calculated spectral profiles (residuals).

(3) To each spectral band add a small linear 'correction', *viz*., a function flexible enough to compensate the fitting residuals but which has some general restrictions that keep these corrections small.

(4) Fit these linear corrections to the differences calculated at step 2.

The 'corrections' may be a linear combination of non-linear functions, for example,

$$c(\nu) = \sum_{i}^{N} A_i(\nu - \nu_{\max})^2 \exp\left[-\left(\frac{\nu - \nu_{\max}}{w_i}\right)^2\right] \qquad (2)$$

where ν is a wavenumber and $\nu_{\max}$ is a position of the band maximum. Having w_i constant and A_i adjustable, the whole function is linear with respect to its parameters. Also, this function can change the line shape considerably, provided that a sufficient number of items are retained (N up to 40). The convenience of this type of correction is that it is symmetric and has zero asymptotes at the origin and the infinities. Such a sum can be assigned to each band and centred at each band centre. The combination of these features of this function keeps it small compared to the non-linear part of the band shape, while at the same time adding the necessary correction to the band shape. The resulting algorithm is implemented in the program we described previously.[1]

Since the corrections are linear the uniqueness of the resolution is preserved as required by condition (b) above. Also, the use of a general method for calculating the confidence intervals (such as the Monte Carlo method) guarantees their reliability for the correction parameters.

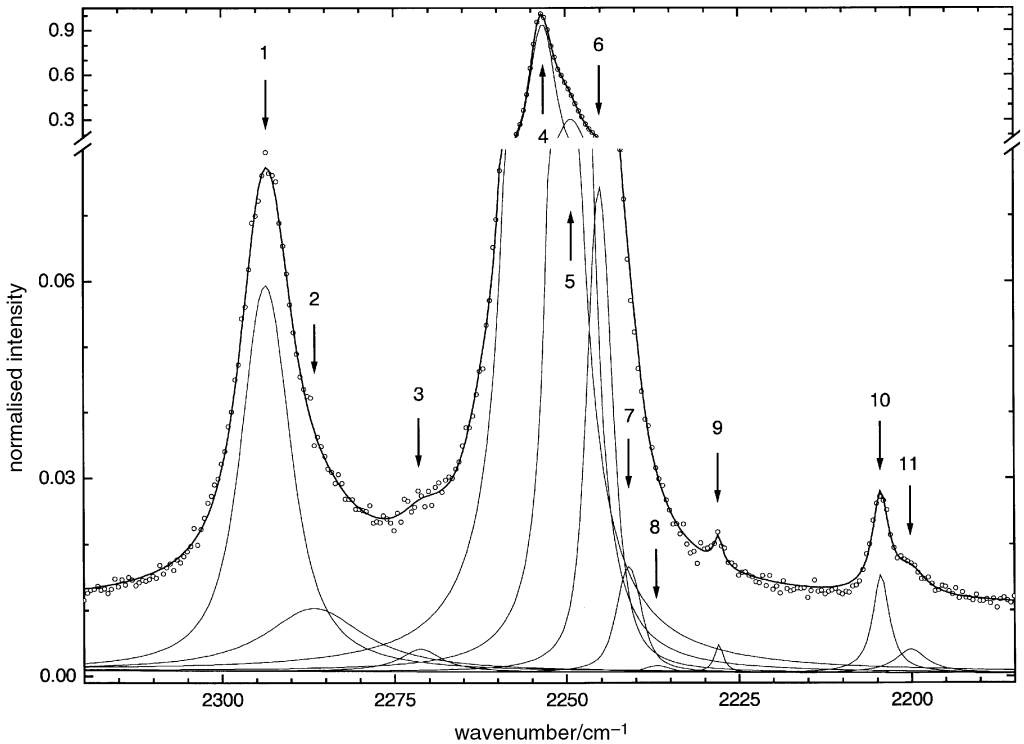

Fig. 3 Set of bands used for resolution of the isotropic Raman spectrum in the range of ν_2 vibrations of liquid acetonitrile at 25 °C. The experimental points (open circles) are shifted upwards by 0.01 units for clarity.

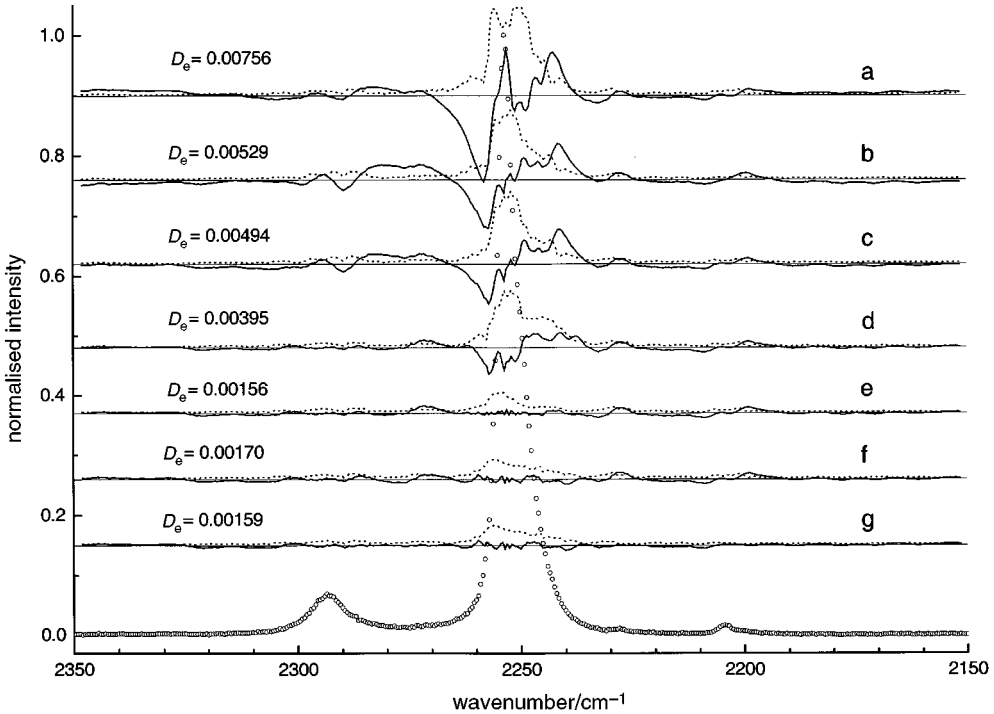

Fig. 4 Development of the shape of bands used for the resolution of the isotropic Raman spectrum in the range of the ν_2 vibrations of liquid acetonitrile at 25 °C. Circles are experimental points; solid lines, the mean of the residuals while the dotted line is its dispersion (see text), both lines multiplied by 5. (a), Lorentz band shape; (b), shape based on Kubo correlation function; (c), the Voigt function band shape; (d), Voigt function with symmetrical linear correction; (e), same but asymmetrical correction; (f), "double sine" band shape; and (g), "double sine" plus auxiliary bands. D_e is the dispersion of approximation.

Results

While liquid acetonitrile (AN) has been investigated in many studies, from spectroscopy to computer modelling,[6–11] the unambiguous interpretation of its vibrational spectra is still challenging. This is because it does not have isolated spectral lines and all lines of interest overlap considerably. However, this chemically important representative liquid is advantageous for study, having a simple and highly symmetrical molecule that bears a significant dipole moment.

The ν_2 vibration, one of the most active in the Raman spectrum, involves the most chemically important C≡N group of the molecule. This is the site of the molecule that is subject to influence by various chemical and physical processes and, consequently, shows the most interesting spectral profile.

Assigning a set of spectral bands

There exists an extensive literature on the assignment of spectral bands in the ν_2 range of the AN spectrum (for representative examples see ref. 6, 9, 10, 12 and 13). The authors use various assumptions concerning the details of the spectral band shapes but the common feature is that the spectrum consists of two fundamental vibrations, ν_2 and $\nu_3 + \nu_4$, and one or more "hot" bands $\nu_2 + \nu_8 - \nu_8$, (the alternative hypothesis of associated AN molecules has been shown to be inconsistent[14]). It is crucial to have a consistent model for comparing results from different investigations because subtle variations in the band shapes can change dramatically the overall band profile. For example, depending on the ratios of the heights of "hot" bands and the fundamental ν_2 vibration, the widths of these bands may vary considerably. Unfortunately, there is not enough information in the Raman spectrum itself to define the number of bands and their relationships unambiguously. Our choice was dictated by having a complex enough model to reproduce all the features in this spectral region while, at the same time, also being simple enough to provide a unique resolution. Our final set of bands is presented in Fig. 3 and consists of the following: (1) Fundamental vibration ν_2: band 4. Four "hot" bands $\nu_2 + n\nu_8 - n\nu_8$ ($n = 1 \cdots 4$): bands 5–8. Their heights were set and fixed according to the Boltzman factor $S_n = S_f$ ($n + 1(\exp[-1.439(n\nu_8/T)]$, where S_n and S_f are the heights of the nth "hot" band and the fundamental band, respectively, ν_8 is the wavenumber of the ν_8 vibration, and T is temperature. We attempted to fit the temperature parameter, and the results were close to the actual temperature of the liquid. A more rigorous approach would require calculating the local temperature in the molecule micro-environment from the ratio of the Stokes and anti-Stokes bands,[15] but this is the subject of a separate study. The bands were considered equi-distant, and their positions were defined by a single parameter $\Delta\nu_h$, where $\nu_n = \nu_f + n\Delta\nu_h$, ν_f is the fundamental band position and $\Delta\nu_h$ is the "hot" band shift. The band shapes were assumed identical to that of the fundamental band.

(2) A combination of bands 1 and 2 describing the $\nu_3 + \nu_4$ vibration.

(3) Several unidentified bands, 3, 9, 10 and 11, required to reproduce the profile correctly. These bands, except band 3, do not substantially affect the main bands of interest (4–8). Besides its significant contribution to the whole profile, the inclusion of the band 3 is justified because its appearance is very pronounced in anisotropic spectra, especially at the higher temperatures employed.

Developing the model for spectral band shapes

The model for the band shapes was developed by starting from the simplest one and gradually changing it to a more sophisticated one. This was effected by steadily adding more features in order to reproduce all the details of the profile. The criterion of the goodness-of-fit, as discussed above, was based on the analysis of the fitting residuals. Generally, the difference between experimental data and the fitted function at each point is a random value, with its own distribution. Even though these distributions are all normal with zero mean, their dispersion may vary from point to point. Therefore, rigorously, it is necessary to accumulate several spectra under exactly the same conditions and then analyse the residuals at

each point, based on the statistics from the different spectra. However, we can assume that the distributions do not change significantly in the neighbourhood of a data point, and the statistics can be accumulated using a single spectrum from several adjacent data points. We thus calculated the following values as the surrogates of the mean and dispersion of the residuals respectively:

$$\overline{\Delta y_k} = \frac{1}{N} \sum_{i=k-N/2}^{k+N/2} [y_i - y^{\text{theor}}(v_i)], \quad k = N/2 + 1 \ldots N^{\text{tot}} - N/2, \quad (3)$$

$$\bar{\sigma}_k = \frac{1}{N} \sum_{i=k-N/2}^{k+N/2} [y_i - y_{\text{theor}}(v_i) - \overline{\Delta y_k}]^2, \quad k = N/2 + 1 \ldots N^{\text{tot}} - N/2, \quad (4)$$

where N is the number of adjacent points used for averaging, y_i their spectral intensity, v_i their corresponding wavenumbers and N^{tot} is the total number of data points. The value of N was varied from 4 to 10 and in this range the final result was not affected qualitatively. The dispersion of approximation is also important as it serves as a gross characteristic of the quality of fit: the lower the dispersion of approximation the better the model. The values of the mean and dispersion calculated in this manner, together with the dispersion of approximation, are shown in Fig. 4 and the process of developing the model is sequentially illustrated.

It is apparent that the simplest band shape, Lorentzian, (curves a) is not a satisfactory description of the spectrum. A more physically realistic model, expressed as a Fourier transformation of the well-known Kubo correlation function,[1] reduces the magnitude of the deviations of the mean from zero but the situation is still far from acceptable (curves b). Also, we found that the Kubo model is computationally inconvenient as the optimisation process was slow and unstable, even when compared with the equally complex model of a Voigt function expressed through its Fourier transform in time domain.[1]

Using the Voigt band shape[1] (fitting in the frequency domain) improves the situation (Fig. 4, curves c) but there is still room for further development. Interestingly, the introduction of the symmetric linear corrections of form (2) (curves d) does not change the picture qualitatively, even when a considerable number of terms (up to 40) is used. This procedure can be visualised as adding the identical correction, symmetric with respect to the band centre, to all the bands 4–8 (Fig. 3). The failure to fit the model properly thus means that the symmetric band shapes are incapable of describing the real spectrum, at least in the framework of the band set chosen.

Considerable progress is achieved when an asymmetric correction is used, Fig. 4e. Here, the correction function (2) has the same number of terms, but they are different and independent on each side of the band. The only restriction left is that the corrections are identical for all five bands 4–8. The resulting correction is shown in Fig. 5.

The surprising feature of this correction is that it is an almost completely odd function. Inset (a) of Fig. 5 shows both "wings" of the function on one side with respect to the band centre, the left "wing" is transformed as $f'(v) = -f(-v)$. This unique property of the correction, together with its shape, suggests two important considerations. First, it can be approximated by some suitable simple analytical function, and, second, since the function is odd, the corresponding correlation function of this vibration is a purely imaginary function. This means that we have a unique opportunity to extract the imaginary part of the vibrational correlation function from the experimental data.

We here use the "double sine" function for fitting the correction:

$$y^{\text{corr}}(v) = -S_0 \sin(w_0[v - v_{\text{max}}])e^{-e_0[v-v_{\text{max}}]^2} - S_1 \sin(w_1[v - v_{\text{max}}])e^{-e_1[v-v_{\text{max}}]^2}, \quad (5)$$

where S_0, w_0, e_0, S_1, w_1 and e_1 are fitting parameters and v_{max} is the band maximum position. This function has a complicated oscillating character that is damped out at higher time values, Fig. 5, inset (b).

The statistics of the fitting of the spectrum, using Voigt band shapes with the "double sine" correction, is shown in Fig. 4f. Indeed, the fit is almost as good as the one with asymmetric correction, but the advantage now is that the band

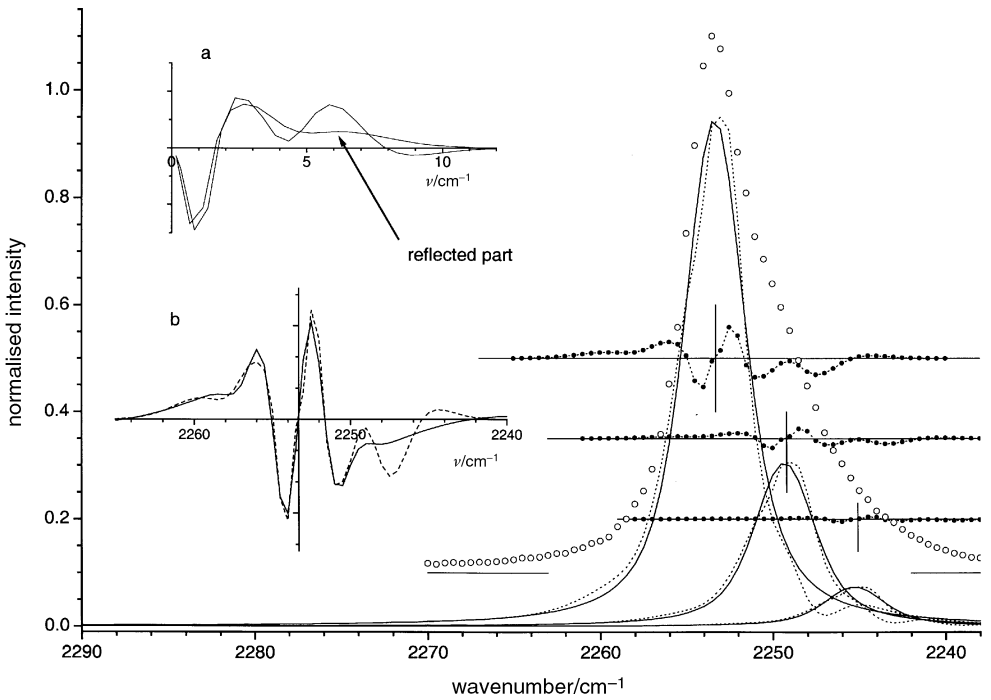

Fig. 5 Asymmetric corrections (filled circles) multiplied by 5, as used in the resolved spectral bands of the ν_2 vibrations of liquid acetonitrile at 25 °C. Open circles, experimental points (shifted upwards by 0.1 units); solid lines, non-linear parts (Voigt function); and dotted lines, bands with linear corrections. Inset (a), correction reflected with respect to the band centre; inset (b), "double sine" fit to the correction (solid line, fitted function; dashed line original correction, see text).

shape reveals more clearly physical information. Specifically, we can now obtain the profiles of both the real *and* imaginary parts of the vibrational correlation function.

The final improvement made to the spectral profile (curves g) is the introduction of the additional bands 2, 3, 9, 10 and 11. These are located well away from the bands of interest, 4–8, and, though they cannot change their shape, they lower noticeably the dispersion of approximation. Additionally, the correction for the apparatus function of the interferometer was introduced by increasing the Gaussian width of each band. The apparatus function was approximated by the Gaussian with width 0.87 cm^{-1}.

Adding the "double sine" part to the model means introducing six more optimising parameters. This makes 11 parameters altogether for the set of bands 4–8. Although the fitting situation is still acceptable, the model has some properties of an overestimated case (see section "Goodness-of-fit"). Indeed, as the calculated confidence intervals showed, the parameters of the "double sine" part can be separated into two groups. While one group, for example, the parameters of the first term, S_0, w_0 and e_0 (eqn. (5)), have standard deviations in the range 5–20% on average, those in the other group, S_1, w_1 and e_1, are much less definite, having confidence intervals of up to 80%. These latter cannot be neglected, however, in that the use of a "single sine" instead of "double sine" worsens considerably the quality of fit. The only correct solution here is in fixing the parameters with high standard deviations, and considering them as constants. This implies the introduction of "predefined" information into the model, similar to information contained in a particular band shape (for example, Lorentzian or Gaussian which have the same number of fitting parameters but the difference in shape is contained in the form of the functions). The fixed parameters are therefore shown in Table 1 without specifying their confidence intervals.

Vibrational correlation functions of liquid AN

Since the spectral band consists of purely even (Voigt function) and purely odd ("double sine") components, its Fourier transform (after normalising, omitting the purely oscillating part and considering positive time) has the form

$$C(t) = \exp\left[-\frac{\sigma_L}{2}t - \frac{\sigma_G^2}{2}t^2\right] + i\left[\frac{1}{2}S_0\sqrt{\frac{\pi}{e_0}}\left(e^{(-1/4e_0)(t-w_0)^2} - e^{(-1/4e_0)(t+w_0)^2}\right) + \frac{1}{2}S_1\sqrt{\frac{\pi}{e_1}}\left(e^{(-1/4e_1)(t-w_1)^2} - e^{(-1/4e_1)(t+w_1)^2}\right)\right] \quad (6)$$

It has been shown both theoretically[16] and experimentally[17–19] that the Raman vibrational correlation function is essentially the sum of auto- and cross-correlation functions, and has both non-vanishing real and imaginary parts. Here we report the experimental complex correlation functions of the ν_2 vibration of the AN molecule at three temperatures, 25, 50 and 75 °C. The parameters of these functions are presented in Table 1, together with their confidence intervals. It is worth stressing that by using our approach essentially *all* possible information is extracted from the experimental spectra and, in fact, the reported correlation functions are the experimental data for the dynamics of the AN molecules.

A detailed analysis of the vibrational correlation functions requires a careful study of modern theories of liquids. Moreover, since these functions are the sum of two unknown parts of the correlation function (auto- and cross-), additional information is needed for picturing specific microscopic motions. However, some general comments on the structure and dynamics can be made.

The ν_{max} and $\Delta\nu_h$ parameters reported in Table 1 are the characteristics of the microstructure of the liquid. The trend towards smaller differences compared to gas phase values is shown with temperature increase (the corresponding gas phase values are $\nu_{max} = 2266.7$ cm^{-1} and $\Delta\nu_h = -4.9$ cm^{-1} [20]). The band position is a characteristic of the strength of the micro-environment influence on the vibrating molecule in the liquid, while the "hot" bands shift provides information on the multi-surface dynamics of the molecule in the condensed phase.

Both real and imaginary parts of the correlation functions are shown in Fig. 6. As expected, the real part of the functions falls more rapidly as the temperature is steadily raised. Also, their shape is changed systematically, the Lorentzian part (the linear term in the real part of eqn. (6)) decreases and the Gaussian part (the quadratic term) increases with temperature. This increase of the Gaussian contribution together with the overall decay rate make the 25 and 50 °C curves cross at short time intervals (Fig. 6). The imaginary parts at all tem-

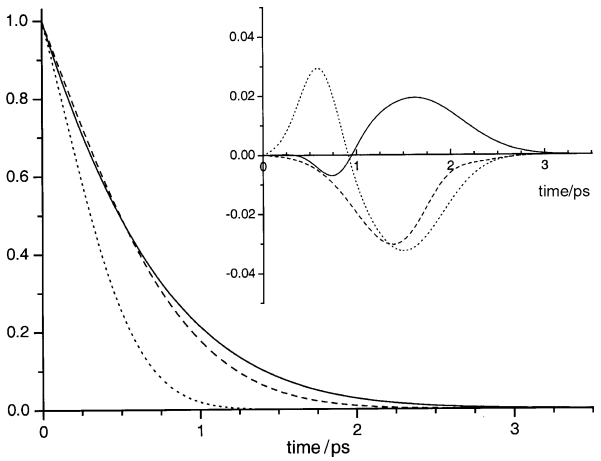

Fig. 6 Real and imaginary (inset) parts of the vibrational correlation function of the ν_2 vibrations of liquid acetonitrile at 25 (solid lines), 50 (dashed lines) and 75 °C (dotted lines). Functions normalised to the value at the origin.

Table 1 Vibrational dynamics parameters of the ν_2 vibration of AN molecules at various temperatures[a]

	25 °C	50 °C	75 °C
ν_{max}/cm^{-1}	2253.262 ± 0.001(0.0%)	2253.490 ± 0.0006(0.0%)	2254.078 ± 0.003(0.0%)
$\Delta\nu_h/cm^{-1}$	−4.10 ± 0.03(0.8%)	−4.62 ± 0.03(0.6%)	−4.61 ± 0.09(2.0%)
σ_L/cm^{-1}	2.61 ± 0.06(2.3%)	2.19 ± 0.06(2.7%)	1.61 ± 0.3(18.3%)
σ_G/cm^{-1}	0.70 ± 0.05(6.7%)	1.13 ± 0.03(2.7%)	1.40 ± 0.12(8.4%)
S_0	0.0017	0.011 ± 0.0007(5.9%)	0.011 ± 0.002(18.0%)
w_0/cm^{-1}	−0.78	−1.44 ± 0.03(1.8%)	−1.50 ± 0.06(3.8%)
e_0/cm^{-1}	0.017	0.10 ± 0.02(11.8%)	0.086 ± 0.043(50.1%)
S_1	0.0078 ± 0.0009(12.0%)	−0.0018	−0.0055
w_1/cm^{-1}	1.64 ± 0.07(4.1%)	−1.90	−0.61
e_1/cm^{-1}	0.14 ± 0.03(22.9%)	0.031	0.022

[a] Relative errors in parentheses.

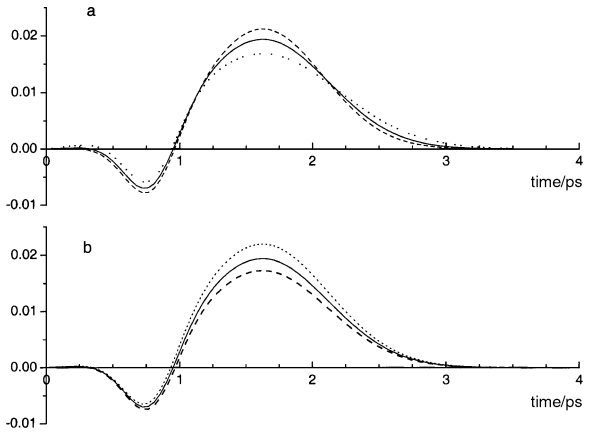

Fig. 7 Effect of the uncertainty in the parameter value for the imaginary part of the vibrational correlation function at 25 °C. (a), parameter e_1 (solid line $e_1 = e_1^{\text{fitted}} = 0.135$, dashed line $e_1 = e_1^{\text{fitted}} - \Delta e_1 = 0.104$, dotted line $e_1 = e_1^{\text{fitted}} + \Delta e_1 = 0.166$); (b), parameter S_1 (solid line $S_1 = S_1^{\text{fitted}} = 0.0078$, dashed line $S_1 = S_1^{\text{fitted}} - \Delta S_1 = 0.0069$, dotted line $S_1 = S_1^{\text{fitted}} + \Delta S_1 = 0.0088$).

peratures of the correlation functions are substantial and the uncertainties in the parameter values do not change the picture qualitatively. An illustration of the influence of the limiting values of the two worst parameters is shown for the 25 °C case in Fig. 7. The imaginary part shows a complicated behaviour with temperature that cannot be described as a simple trend. Its parameters are obviously not related to physical characteristics in a clear way and any explanation will thus require a detailed analysis of the theory. Additionally, since the shape of the imaginary part differs dramatically at all three temperatures more experimental data at intermediate temperatures will be required to clarify their behaviour.

One of the most elaborate models for the vibrational correlation function can be found in the publications of Bratos *et al.*[16,21,22] The final formulae for vibrational correlation functions are provided for the limiting cases of "slow" and "fast" modulation. Neither extreme case can fit the experimental correlation function satisfactorily, and this means that the intermediate case should be used. Unfortunately, obtaining the applicable form for this case requires substantial effort, including specification of the interparticle potential and many other assumptions. This, together with an analysis of other theories of vibrational relaxation (*e.g.*, the "stretched exponential" model),[4,5] will be the subject of a future publication.

Conclusions

Detailed quantitative data on the dynamics of acetonitrile molecules in liquid phase is reported here. Using general assumptions, the parameters of the structure and dynamics have been obtained, together with their statistical characteristics. This information can be used for testing various theories of liquids and work in this direction is currently in progress. In particular, because of the behaviour of the imaginary part of the correlation function at 25, 50 and 75 °C, measurements at intermediate temperatures should be very interesting.

Experimental

Acetonitrile was distilled four times, initially twice from P_2O_5, then from K_2CO_3 before final distillation. Raman spectra were measured using 0.5 cm^{-1} data point intervals on a Ramanor U-1000 spectrometer (Jobin Yvon) with a resolution of 0.15 cm^{-1}. Full details are given in ref. 1 and 23.

Acknowledgements

The authors thank Dr V. P. Gnezdilov, Kharkov Institute for Low Temperatures, Ukraine, for experimental assistance. D. N. thanks the Royal Society of Chemistry for a Travel Grant for International Authors that made possible effective collaboration with Dr T. R. Griffiths during the final stage of this report.

References

1 T. R. Griffiths, D. A. Nerukh and A. Eremenko, *Phys. Chem. Chem. Phys.*, 1999, **1**, 3199.
2 W. H. Press, S. A. Teukolsky, W. T. Vetterling and B. P. Flannery, *Numerical Recipes in C: The Art of Scientific Computing*, Cambridge University Press, Cambridge, 1992.
3 W. G. Rothschild, *Dynamics of Molecular Liquids*, Wiley, New York, 1984.
4 C. H. Wang, *Spectroscopy of Condensed Media, Dynamics of Molecular Interactions*, Academic Press, New York, 1985.
5 S. A. Kirillov, *J. Mol. Liq.*, 1998, **76**, 35.
6 S. Hashimoto, T. Ohba and S. Ikawa, *Chem. Phys.*, 1989, **138**, 63.
7 B. Guillot, P. Marteau and J. Obriot, *J. Chem. Phys.*, 1990, **93**, 6148.
8 P. O. Westlund and R. M. Lynden-Bell, *Mol. Phys.*, 1987, **60**, 1189.
9 A. Morresi, P. Sassi, M. Paolantoni, S. Santini and R. S. Cataliotti, *Chem. Phys.*, 2000, **254**, 337.
10 A. Morresi, P. Sassi, M. Ombelli, G. Paliani and R. S. Cataliotti, *Phys. Chem. Chem. Phys.*, 2000, **2**, 2857.
11 E. Guardia and R. Pinzon, *J. Mol. Liq.*, 2000, **85**, 33.
12 C. Breuillar-Alliot and J. Soussen-Jacob, *Mol. Phys.*, 1974, **28**, 905.
13 D. Jamroz, J. Stangret and J. Lindgren, *J. Am. Chem. Soc.*, 1993, **14**, 6165.
14 D. A. Nerukh, *Interparticle interactions and dynamics of molecules in electrolyte solutions of n-hexanol and acetonitrile by vibrational spectroscopy*, PhD Thesis, Kharkov, 1996.
15 E. B. Wilson, Jr., J. C. Decius and P. C. Cross, *Molecular Vibrations*, McGraw Hill, New York, 1955.
16 S. Bratos and G. Tarjus, *Phys. Rev. A*, 1981, **24**, 1591.
17 K. Oehme and K. Klostermann, *Chem. Phys. Lett.*, 1990, **170**, 103.
18 K. Oehme and K. Klostermann, *J. Chem. Phys.*, 1989, **91**, 2124.
19 K. Oehme, G. Rudakoff and and K. Klostermann, *J. Chem. Phys.*, 1985, **83**, 1499.
20 F. W. Parker, A. H. Nielsen and W. H. Fletcher, *J. Mol. Spectrosc.*, 1957, **1**, 107.
21 S. Bratos and E. Marechal, *Phys. Rev. A*, 1971, **52**, 1078.
22 G. Tarjus and S. Bratos, *Phys. Rev. A*, 1984, **30**, 1087.
23 S. A. Eremenko, O. N. Kalugin and D. A. Nerukh, *Proc. Kharkov Univ., Chemistry*, 1997, **1**, 34.